



Effect of surface chemistry and content of nanocrystalline cellulose on removal of methylene blue from wastewater by poly(acrylic acid)/nanocrystalline cellulose nanocomposite hydrogels

Seyedeh-Arefeh Safavi-Mirmahalleh · Mehdi Salami-Kalajahi · Hossein Roghani-Mamaqani

Received: 31 January 2019 / Accepted: 6 May 2019 / Published online: 9 May 2019
© Springer Nature B.V. 2019

Abstract Nanocrystalline cellulose (NCC) was modified with (3-aminopropyl)triethoxysilane (APTES) and hexadecyltrimethoxysilane (HDTMS) to obtain NCC-APTES and NCC-HDTMS respectively. The modification was confirmed by Fourier transform infrared (FT-IR) spectroscopy, X-ray diffraction (XRD) spectroscopy, thermogravimetric analyses (TGA), dynamic light scattering and zeta potential analyses. A series of poly(acrylic acid) (PAA)/NCC, PAA/NCC-APTES, and PAA/NCC-HDTMS hydrogel nanocomposites with various amounts of nanoparticles were synthesized by in situ radical polymerization method. Nanocomposites were characterized using XRD, TGA and field emission scanning electron microscopy. Also, swelling behavior of hydrogel nanocomposites showed that

NCC and NCC-APTES helped swelling of hydrogels whereas CNN-HDTMS decreased swelling ratio. The hydrogel nanocomposites were also used as adsorbents for removal of methylene Blue from aqueous solution at different pH values. Results showed that the adsorption capacity for dye increased with increasing pH and contact time. Introducing NCC into hydrogel nanocomposite network affected adsorption capacity. Finally, adsorption kinetics was studied by three kinetic models including pseudo-first-order, pseudo-second-order and intra-particle diffusion models.

Keywords Nanocrystalline cellulose · Nanocomposite hydrogels · Dye removal · Adsorption · Methylene blue

Electronic supplementary material The online version of this article (<https://doi.org/10.1007/s10570-019-02490-1>) contains supplementary material, which is available to authorized users.

S.-A. Safavi-Mirmahalleh · M. Salami-Kalajahi (✉) · H. Roghani-Mamaqani (✉)
Department of Polymer Engineering, Sahand University of Technology, P.O. Box 51335-1996, Tabriz, Iran
e-mail: m.salami@sut.ac.ir

H. Roghani-Mamaqani
e-mail: r.mamaghani@sut.ac.ir

S.-A. Safavi-Mirmahalleh · M. Salami-Kalajahi · H. Roghani-Mamaqani
Institute of Polymeric Materials, Sahand University of Technology, P.O. Box 51335-1996, Tabriz, Iran

Introduction

Organic dyes are widely used in various industries such as textile dyeing (Patil et al. 2010), printing (Seema et al. 2018), cosmetics (Guerra et al. 2018), paper making (Blus et al. 2014), etc. Dyes in wastewater are harmful to environment and cause health problems because of the toxicity and difficulty of degradation. So, the removal of dyes from wastewater is important. Many methods have been developed to remove dyes such as coagulation-flocculation (Panswed and Wongchaisuwan 1986), oxidation (Malik and Saha 2003), membrane separation (Ciardelli

et al. 2001), electrochemical processes (de Paiva et al. 2018), and adsorption (Mall et al. 2005). Among them, adsorption is an effective process for the removal of dyes because of its low cost, easy technical access and simplicity of design (Wang and Peng 2010; Cheng et al. 2016; Zheng and Wang 2009; Zhou et al. 2011). Different types of adsorbents are commonly used to remove dyes such as activated carbon (Luo and Zhang 2009), clays (Almeida et al. 2009), natural zeolites (Wang et al. 2010), industrial byproducts and wastes (Ahmad et al. 2009), natural polymers (Annadurai et al. 2002), and hydrogels (Soleimani et al. 2018).

It was well-known that cross-linked polymeric materials especially hydrogels with functional groups such as carboxylic acid, hydroxyl, amine and sulfonic acid groups can be used as complexing agents for removal of dyes from aqueous solutions (Bekiari et al. 2008; Yetimoğlu et al. 2007; Rahchamani et al. 2011; Atta et al. 2012). When hydrogels encounter aqueous solutions, they adsorb and keep the dissolved materials (Akkaya et al. 2009; Rashidzadeh et al. 2015; Noein et al. 2017; Modarresi-Saryazdi et al. 2018). This water absorption is possible due to hydrophilic groups that establish hydrogen bonding with water (Abdollahi et al. 2016; Fallahi-Samberan et al. 2019) or electrostatic interactions (Lu et al. 2015a, b; Abdollahi et al. 2018). The water absorption process can be fine-tuned for diverse applications such as removal of dyes and heavy metals from wastewaters (Lu et al. 2015a; Li et al. 2011; Kasgöz and Durmus 2008) and drug delivery systems (Yassin et al. 2015; Fallahi-Samberan et al. 2018; Dehghani et al. 2019). This is achieved by controlling the amount of water uptake through changes in pH or temperature of the medium (Banaei and Salami-Kalajahi 2015; Hernandez-Martínez et al. 2018; Nikravan et al. 2018a, b). Special structure of hydrogels allows the diffusion of solutes into the network. Also, hydrogel possesses a lots of ionic or nonionic functional groups those can absorb or trap ionic dyes from wastewater (Liu et al. 2010).

Incorporating natural materials into hydrogels affects their swelling behavior and adsorption capacity. Carbohydrate polymers are more attractive than synthetic ones due to their unique properties such as good hydrophilicity, biodegradation and biocompatibility (Sharma et al. 2015; Vakili et al. 2014; Abdeen and Mohammad 2014; Golshan et al. 2017). Cellulose is the most available and naturally renewable polysaccharide with unique physical and mechanical

properties (Varaprasad and Jayaramudu 2017; Zhou et al. 2011). It contains hydroxyl groups those can help adsorption of water and dye molecules (Suo et al. 2007; Ibrahim et al. 2007). Many cellulose derivatives such as nanocrystalline cellulose (NCC) (Yang et al. 2012), carboxymethyl cellulose (CMC) (Nath and Dolui 2018) and hydroxyethyl cellulose (HEC) (Wang et al. 2010) have been used for synthesizing hydrogels adsorbents with acrylic acid. Zhu et al. reported the preparation of palygorskite/poly(acrylic acid) (PAA) nanocomposite hydrogels for adsorbing cationic basic dye (Zhou et al. 2011). Liu et al. reported β -cyclodextrin/PAA-grafted graphene oxide (β -CD/PAA/GO) hydrogels for removal of cationic dye, methylene blue (MB), from aqueous solution through electrostatic attraction, host–guest supramolecular interactions, and π - π conjugation interactions (Liu et al. 2014). Solpan et al. prepared poly(acrylamide-co-acrylic acid) poly(AAm-co-AA) hydrogel by irradiating with gamma radiation and applied it for the adsorption of cationic dyes such as Safranin-O (SO) and Magenta (M) (Şolpan et al. 2003). Singh et al. synthesized a novel biodegradable multifunctional superabsorbent hydrogels (SAHs) for adsorption of crystal violet (CV) and MB (Singh and Singhal 2015). Qi et al. fabricated adsorbents by cross-linking copolymerization of acrylamide (AAm) and diallyldimethylammonium chloride (DADMAC) in the presence of salean and used them for efficient removal of dyes and heavy metal ions (Qi et al. 2018). Zendeheel et al. prepared a semi-interpenetrating hydrogel composed of poly(AAm-co-AA) and poly(vinyl alcohol). Then, the adsorption ability of the hydrogel for removal of MB from aqueous solutions was investigated (Zendeheel et al. 2010). Zarezadeh-Mehrzi et al. used the octavinyl polyhedral oligomeric silsesquioxane nanoparticle (OVS) as a cross-linker for the PAA/OVS hydrogel with 3D crosslinking network via radical polymerization. The adsorption properties of the obtained nanocomposite hydrogels were tested for MB as a model cationic dye (Zarezadeh-Mehrzi et al. 2017).

In this study, crosslinked PAA/NCC nanocomposite hydrogels with different amounts of NCC are prepared by in situ free radical polymerization in aqueous media and used in removal of MB. To investigate the effect of surface modification on swelling behavior of nanocomposite hydrogels and dye removal capacity, NCC is used in pristine state

and also, modified with (3-amino)propyltriethoxysilane (APTES) (NCC-APTES) and hexadecyltrimethoxysilane (NCC-HDTMS). All nanocomposite hydrogels are used as MB absorbent in different pH values because MB is the most commonly used cationic dye in industries and its effective removal from wastewater is very important. The high surface area and surface functional groups of nanoparticles strongly suggest affecting the adsorption capacity of hydrogels. Finally, the adsorption kinetics of MB by different nanocomposite hydrogels are studied using different adsorption kinetics models.

Experimental methods

Modification of NCC by APTES and HDTMS

For surface modification, NCC (0.7 g) was dispersed in ethanol (70 mL) ultrasonically to reach a homogeneous dispersion at 60 °C. After purging nitrogen, silane coupling agent (2.8 mL) (12.0 mmol APTES and 7.2 mmol HDTMS) was added dropwise during 2 h and the reaction was continued for 3 h. For purification, the obtained suspension was centrifuged (10,000 rpm) and washed with a solution of water/ethanol three times. The final product was then freeze-dried overnight (Zhang et al. 2012).

Synthesis of PAA/(modified) NCC nanocomposite hydrogels

The hydrogels were prepared by free radical polymerization of AA in NCC or modified NCC suspension using KPS as initiator. The nanocomposite hydrogels were synthesized by varying the amount of (modified) NCC from 1.0 to 3.0 wt% (with respect to the amount of monomer) at constant amount of crosslinker (*N,N'*-methylenebis(acrylamide), MBA) and initiator (KPS). Typically, a mixture of water (10 mL), AA (2.36 mL, 34.4 mmol), and (modified) NCC was prepared and the mixture was homogenized to ensure the NCC was suspended uniformly. Then, MBA (0.26 g, 1.7 mmol) in 5 mL water was added to the solution and heated in an oil bath at 60 °C. After replacing atmosphere by nitrogen, KPS solution (0.06 g, 0.2 mmol) was added and reaction was performed for 24 h. Final product was washed with distilled water for 3 days and the sample was dried in vacuum at 50 °C. For NCC-

HDTMS containing hydrogels, ethanol was used as solvent. Table 1 shows the sample coding for modification and polymerization steps.

Evaluation of swelling behavior

The swelling behavior of nanocomposite hydrogels was evaluated by immersing dried hydrogels in aqueous media at different pH values. Then, the sample was taken out at certain time intervals, blotted with filter paper to remove water on the surface and weighted. The swelling ratio (*SR*) for each sample was calculated via Eq. (1) (Anirudhan and Rejeena 2012):

$$SR = \frac{W_s - W_d}{W_d} \quad (1)$$

where W_s and W_d are the weights in swollen and dry states respectively.

Adsorption studies

All adsorption experiments were carried out at ambient temperature. Aqueous solutions of MB at two pH values (1 and 8) were used to investigate the adsorption kinetics and isotherms. Hydrogels (0.05 g) was immersed in MB solution (100 mL, 5 mg/L) and sampling was performed at pre-determined time intervals by taking out a 1 mL aqueous solution and replacing fresh water. The concentration of MB was measured by a UV–Vis–NIR spectrophotometer at 662.5 nm for pH = 1 and 665 nm for pH = 8. The adsorption capacities of hydrogels (q_e , mg dye/g hydrogel) were calculated via Eq. (2) (Akkaya et al. 2009).

$$q_e = \frac{(C_i - C_e)V}{m} \quad (2)$$

where C_i and C_e are the concentrations of MB in the initial solution and the aqueous phase after adsorption respectively, V is the volume of the dye solution and m is the weight of hydrogel.

Results and discussion

In this study, we have prepared a series of PAA/(modified) NCC nanocomposite hydrogels containing different amounts of (modified) NCCs using free radical polymerization in the presence of MBA as

Table 1 Sample coding for modification and polymerization steps

Sample	Description
NCC-APTES	NCC modified with APTES
NCC-HDTMS	NCC modified with HDTMS
HNx	PAA/NCC nanocomposite hydrogel with × wt% nanoparticle
HAx	PAA/NCC-APTES nanocomposite hydrogel with × wt% nanoparticle
HHx	PAA/NCC-HDTMS nanocomposite hydrogel with × wt% nanoparticle

cross-linker. At first, we modified NCC with APTES and HDTMS. Then, the free radical polymerization was performed to produce nanocomposite hydrogels those were used for adsorption of MB dye. The preparation route of nanocomposite hydrogels and adsorption behavior are shown in Scheme 1.

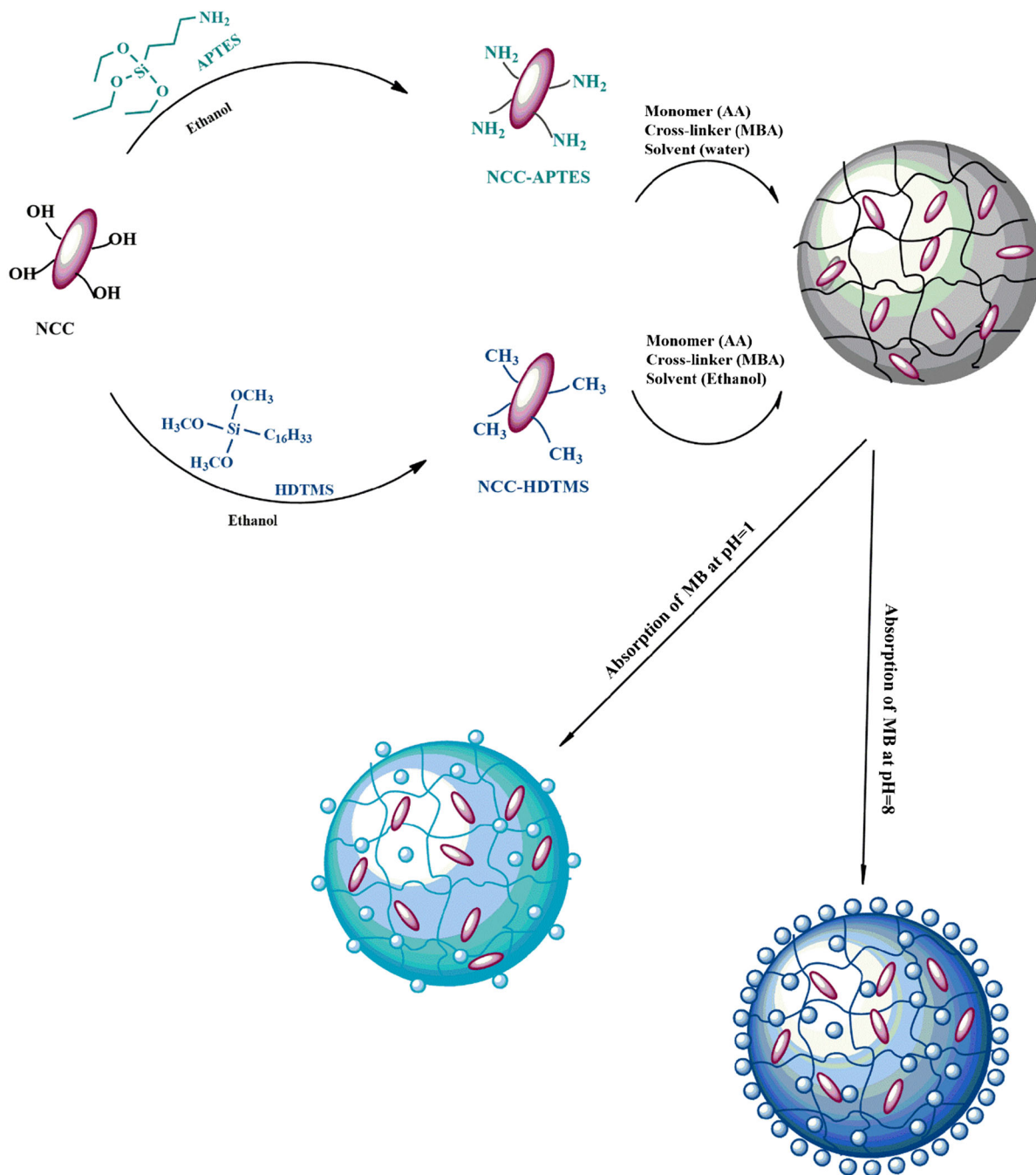
Preparation of NCC and its modification

To confirm the success of the preparation and modification of NCC, various analyses were performed. As observed by FE-SEM images (Figure S1), MCC have a length of 10–50 μm and a diameter of 10–25 μm. These large sized microcrystals are made from microfibrils with strong hydrogen bonding. MCC was converted to NCC through acid hydrolysis. NCC is rod-like with length of 100–200 nm and diameter 10–20 nm. NCC has a coagulated and aggregated morphology due to its high surface area and strong hydrogen bonding (Habibi 2014). Figure S2 shows the FT-IR spectra of MCC, NCC, NCC-APTES and NCC-HDTMS. According to the results, due to the intracellular hydrogen bonding of cellulose, the broad peak at 3200–3550 cm⁻¹ is assigned to O–H groups (Haqani et al. 2017) and C–H stretching vibrations are observed at 2850–2950 cm⁻¹ (Panahian et al. 2014). Peak at 1645 cm⁻¹ originates from –OH stretching of water molecules adsorbed to the structure of nanoparticles (Mazlita et al. 2016) and peaks appearing from 1310 to 1370 cm⁻¹ are due to the bending vibration of the C–H and C–O groups in the polysaccharide rings in cellulose (Kargarzadeh et al. 2012). Also, peak at 1050–1110 cm⁻¹ is due to the bending vibration of the C–O–C (Yang 2017). The characteristic peak of β-glucosidic bond between the glucose rings and the cellulose chains are observed at 896–900 cm⁻¹ (Yang 2017; Shankar and Rhim 2016). After modification of NCC with APTES, new peaks appeared at 3320 and 3290 cm⁻¹ related to stretching and at 1564 cm⁻¹ due to bending vibrations of –NH₂

groups (Gao et al. 2009; Sharifzadeh et al. 2016). The typical absorption peaks of the Si–O–Si bonds of the siloxane compounds were overlapped by the cellulose bands due to C–O bending modes (Gao et al. 2009). In NCC-HDTMS, observed peaks at 2925 and 2854 cm⁻¹ represent the symmetric and asymmetric stretching vibrations of CH₂ groups (Amirshaqai et al. 2014). This indicates that the long-chain alkyl groups (–C₁₆H₃₃) of HDTMS were successfully grafted on NCC surface (Gao et al. 2009; Luo et al. 2017). The XRD patterns of MCC, NCC, NCC-APTES and NCC-HDTMS are shown in Figure S2. NCC displays four diffraction peaks at 15.1 (110), 16.5 (110), 22.7 (200), and 34.6° (004) those are typical peaks of cellulose (Kumar et al. 2014). Peaks at 15.1 and 16.5° show the cellulose type I structure. Crystallinity index (*I_c*) of samples was calculated according to Segal peak height method via Eq. (3) as follows:

$$I_c(\%) = \frac{I_{(200)} - I_{am}}{I_{200}} \times 100 \quad (3)$$

where *I*₍₂₀₀₎ represents combined crystalline and amorphous parts of cellulose (peak intensity at around 22.7°) and *I*_{am} represents the amorphous part of cellulose (peak intensity at around 18°) (Segal et al. 1959; Ahvenainen et al. 2016). According to the results, crystallinity of MCC, NCC, NCC-APTES and NCC-HDTMS was calculated 79.3, 82.7, 80.9 and 80.7% respectively. Decreasing the NCC crystallinity index after modification is associated to the APTES and HDTMS amorphous parts. However, XRD peaks of modified samples showed that the structure of NCC nanoparticles is retained and different processes including modification and acid washing did not disturb the crystalline structure. The size of crystallites for different samples was also calculated according to Scherrer Equation (Bhatia et al. 2017; Pirayesh et al. 2018):



Scheme 1 Fabrication process of nanocomposite hydrogels those are used in dye absorption

$$D = \frac{K\lambda}{B \cos \theta} \quad (4)$$

where θ is the diffraction angle, K is the Scherrer constant, λ is the X-ray wavelength and β is the peak width at half of maximum intensity in radians. The

crystallite size for MCC, NCC, NCC-APTES and NCC-HDTMS were 3.9, 4.1, 4.0, and 3.6 nm respectively. Higher crystallite size of NCC compared to MCC caused by degradation of smaller crystallites and growth of incomplete crystallites during the MCC acid

hydrolysis process (Maiti et al. 2013). The NCC surface modification led to the dissociation of the hydrogen bonds in its structure which prevented aggregation of NCCs; thereby, the size of crystallites was decreased after surface modification.

According to TGA results (Fig. 1), weight loss of 79.1% in NCC is due to the loss of water in glucose units in the main chain, the break of the main molecular backbone and the failure of the C–O and C–C bands. The small particle size and high effective surface area of NCC led to its degradation at low temperatures. Also, amorphous chains on the surface of NCC degraded at lower temperatures and reduced its thermal stability. Degradation of NCC occurred at one step and there is no degradation step at temperatures between 150 and 200 °C which is due to the absence of the sulfate groups in NCC (Cha et al. 2012). So, repeated centrifugation and ultrasonic processes and adding NaOH to the solution resulted in sulfate free NCC product. After modification with APTES and HTDMS, weight loss reduced to 69.6 and 72.7% respectively. The thermal stability of nanoparticles was improved due to the crosslinking of the APTES and HDTMS via silanol groups on the surface of the nanoparticles.

DLS was performed to investigate the changes in size of nanoparticles after each step of modifications. To this end, a 1 mg/mL solution of MCC, NCC, NCC-APTES and NCC-HDTMS was analyzed at room temperature as results are depicted in Fig. 1. Z-average particle size of MCC, NCC, NCC-APTES and NCC-HDTMS was reported 503.6, 304.7, 45.7 and 121 nm respectively. It was observed that NCC has a smaller particle size than MCC due to the failure of glucose bands during acid hydrolysis and physical reduction of the dimensions (Nilsson 2017). The smaller size of modified samples indicated the breakdown of hydrogen bonding in NCC structure. In other words, surface modification of the nanoparticles prevented the accumulation of NCCs resulting in a decrease in particle size. It was also noted that NCC-HDTMS samples showed larger particle size than NCC-APTES due to the dispersion forces in NCC-HDTMS those acted as a driving force for aggregation. On the other hand, a narrow size distribution was observed in all samples. The PDI values obtained for MCC, NCC, NCC-APTES and NCC-HDTMS were 0.02, 0.07, 0.01 and 0.007 respectively. Also, the Zeta potential for MCC, NCC, NCC-APTES and NCC-

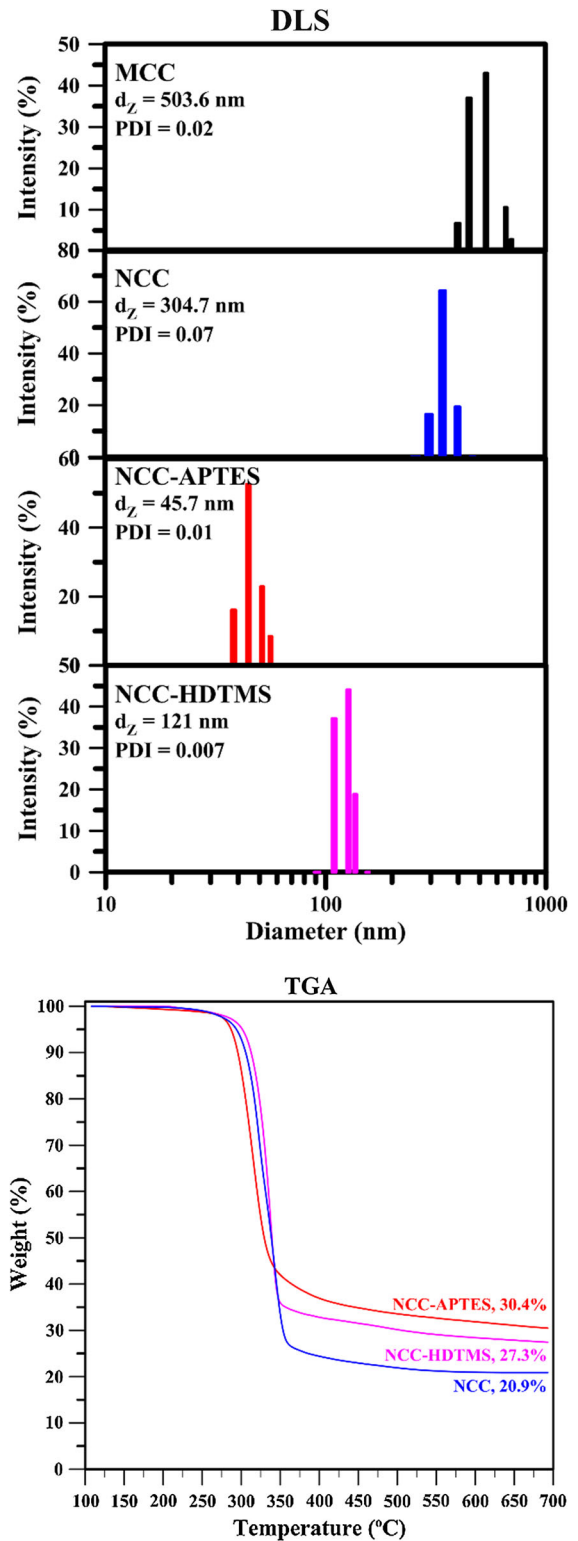


Fig. 1 TGA thermograms and DLS results of MCC, NCC, NCC-APTES and NCC-HDTMA nanoparticles

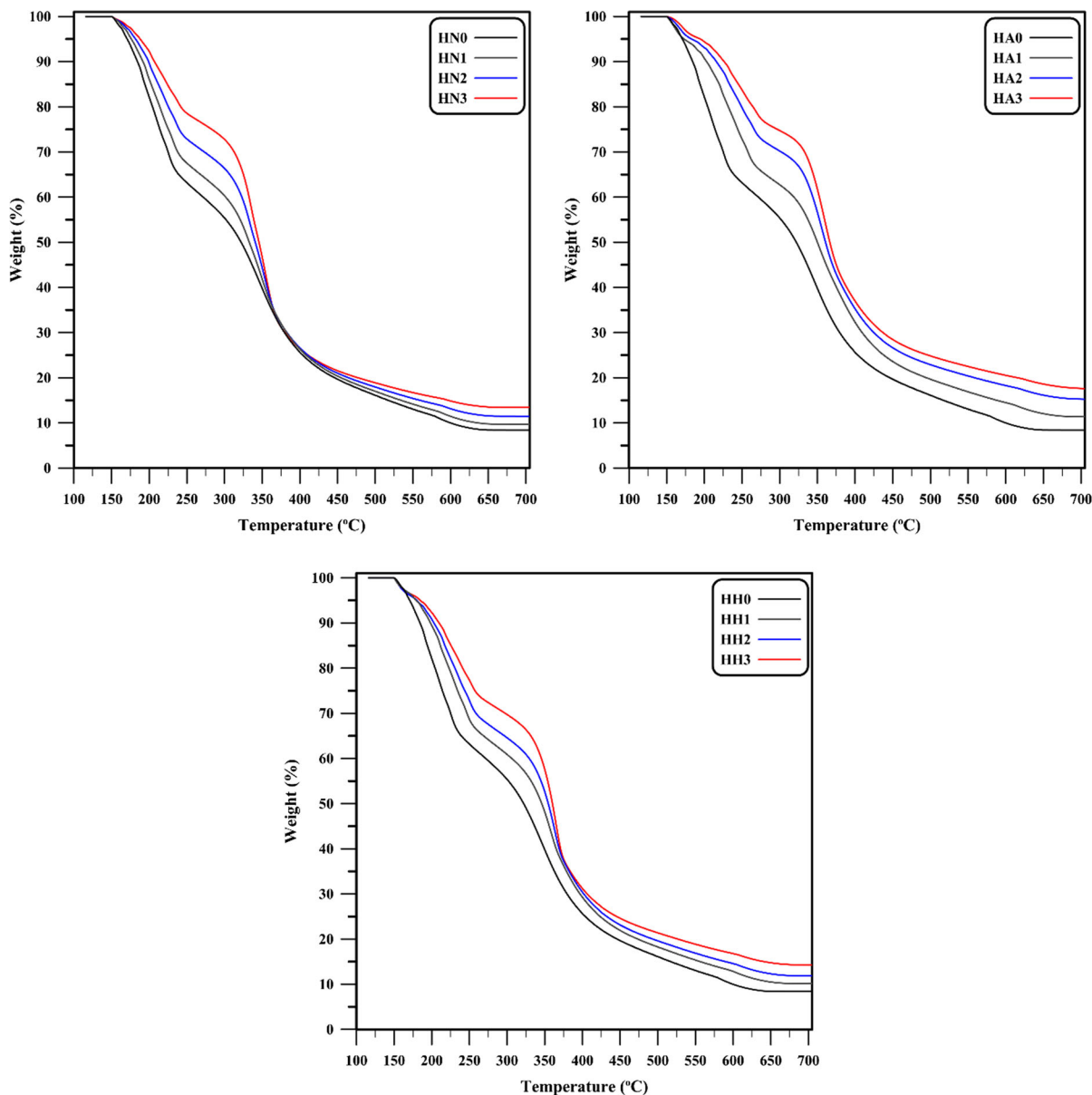


Fig. 2 TGA thermograms of nanocomposite hydrogels prepared with different amounts of NCC, NCC-APTES and NCC-HDTMS

HDTMS were calculated to be -16.4 , -19.6 , $+2.2$, and -2.1 respectively (Figure S2). The higher charge on NCC surface than MCC is due to acid hydrolysis process and the increase of the surface which led to an increase in OH groups on the surface and thus, increasing negative charge absorption rate on the surface (Melo et al. 2018). On the other hand, after modification of NCC with HDTMS, the charge on the surface was reduced, which is explained by replacing OH groups with carbon chains. In NCC-APTES, the

zeta potential showed a positive amount that is related to the $-\text{NH}_2$ groups of the APTES those can absorb protons in aqueous medium (Yamada et al. 2006).

As a conclusion, surface modification of NCC was performed successfully using hydroxyl groups on its surface. Controlling the hydrophilicity and hydrophobicity of NCC is very important to achieve the best compatibility between NCC and the polymer matrix. In this regard, we used two modification agents (APTES and HDTMS) to produce hydrophilic and

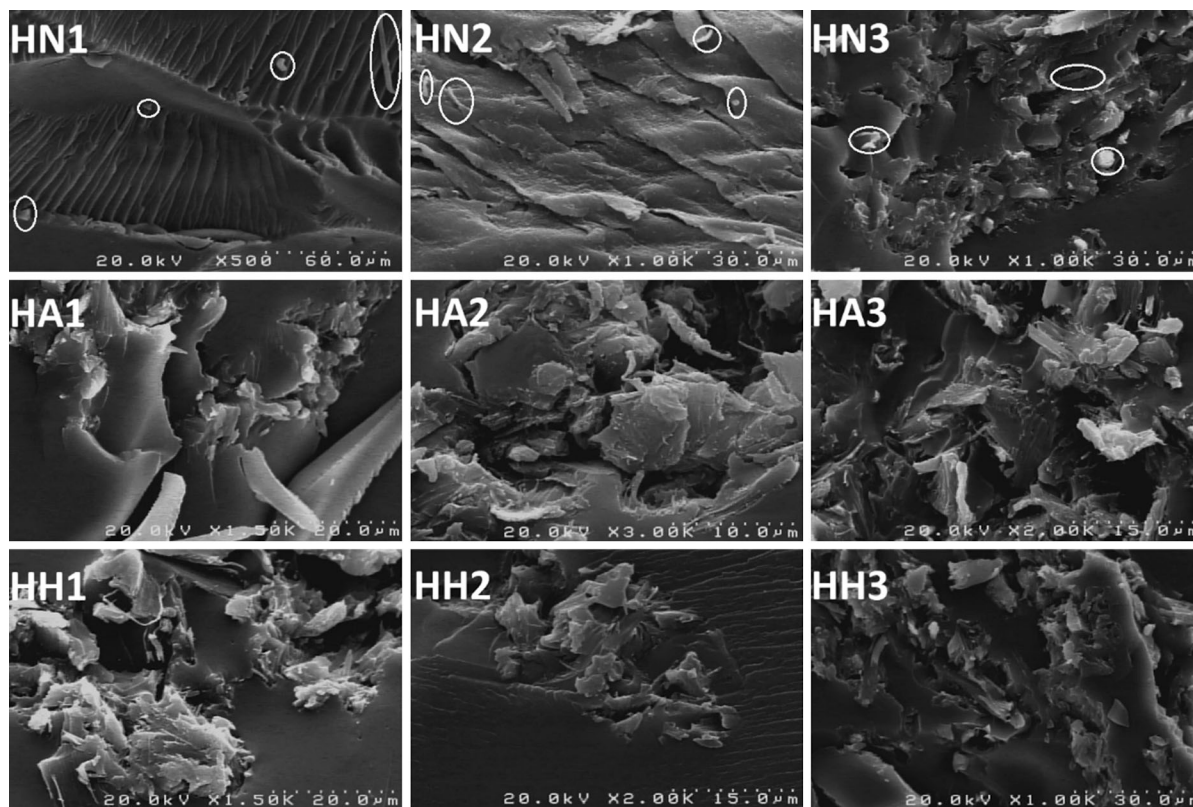


Fig. 3 FE-SEM images of NCC/PAA, NCC-APTES/PAA, and NCC-HDTMS/PAA nanocomposite hydrogels

hydrophobic NCCs those were incorporated in PAA matrix to fabricate nanocomposite hydrogels.

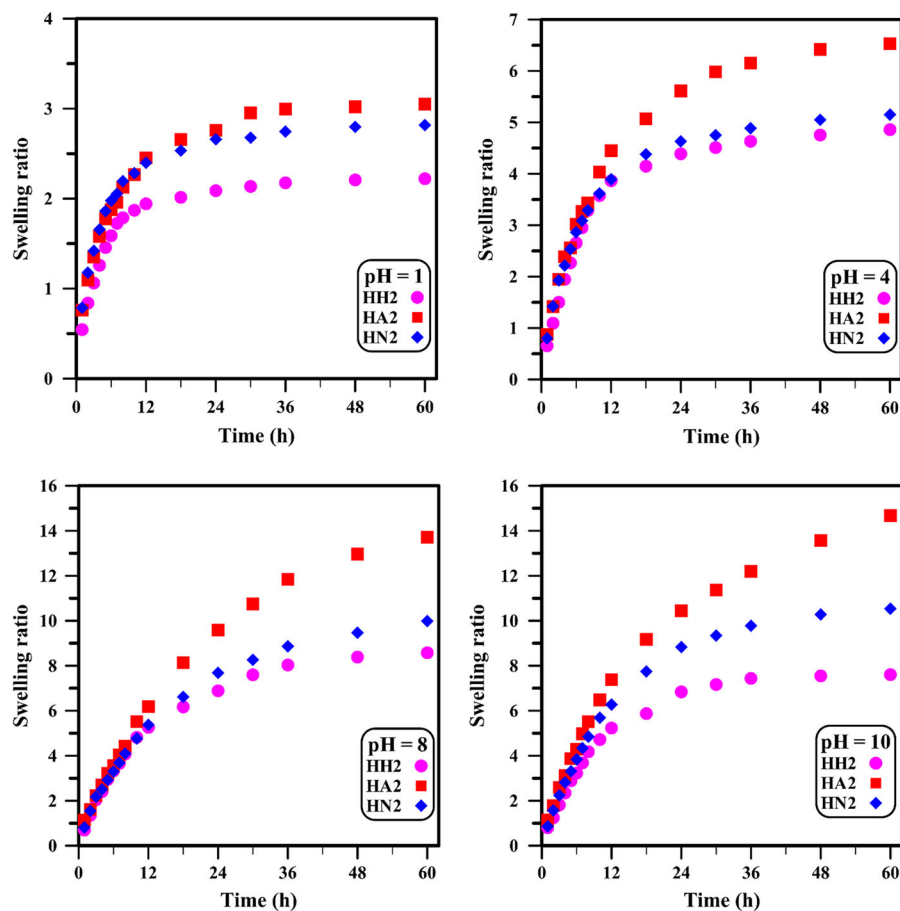
Fabrication and characterization of nanocomposite hydrogels

To investigate the properties of nanocomposite hydrogels, different analyses were utilized. The thermal degradation behavior of the nanocomposite hydrogels was studied in the temperature range of 100–700 °C under nitrogen atmosphere as results are presented in Fig. 2 and summarized in Table S1. PAA weight loss occurred in two stages. The first decomposition of PAA occurred with release of H₂O, CH₄ and monomer (acrylic acid) in the range of 150–330 °C and the second weight loss occurred between 300 and 600 °C due to the separation of the short chain of acrylic acid from the main chain (degradation of the backbone). It is clearly showed that incorporation of NCC into PAA hydrogel and interaction of NCC with PAA chains enhanced the thermal stability of the hydrogel even insignificant. This may originate from low thermal

stability of NCC. The $T_{d,max}$ of HN0 was about 349 °C and shifted to higher temperatures by increasing NCC content. Similar trends were observed for HA and HH nanocomposite hydrogels where increasing the amount of nanoparticles from 1 to 3 wt% led to better thermal stability. On the other hand, it was observed that the HH hydrogels had a higher degradation temperature than HN and HA due to modification with HDTMS.

XRD diffractograms for different nanocomposite hydrogels are shown in Figure S3. XRD patterns for hydrogels were found to be dramatically affected by the presence of PAA, where only a single broad peak ranging from 10° to 30°, characteristic of the amorphous domain, was observed. This observation could be explained by the small content of nanoparticles in the hydrogel nanocomposites (Hou et al. 2017) and appropriate dispersion of nanoparticles in polymeric matrix (Moqadam et al. 2018). FE-SEM images of HN, HA, and HH nanocomposite hydrogels are presented in Fig. 3. All nanoparticles are dispersed in matrix in aggregated form. On the other hand, the

Fig. 4 Swelling ratio of HN2, HA2 and HH2 nanocomposite hydrogels at different pH values



surface of nanocomposites is rough and has many undulations and folds. Due to the uneven surface morphology, the surface area of these hydrogels has increased and water molecules have penetrated the structure of hydrogels (Luo et al. 2018). Moreover, the increase of NCC values leads to the filling the hydrogels structure that may result in lower water diffusion to the structure of hydrogels (Bashir et al. 2017). However, in HH nanocomposites the agglomerations are bigger than other nanocomposite hydrogels. This can be ascribed to hydrophobic surface of NCC-HDTMS nanoparticles where dispersion forces are the main driving force to make bigger agglomeration.

Swelling behavior of nanocomposite hydrogels

The swelling ratio was monitored for different nanocomposite hydrogels via gravimetry approach in pre-determined time intervals at different pH values as

results are illustrated in Figs. 4 and S3–S5. Figure 4 shows the swelling ratio for HN2, HA2 and HH2 nanocomposite hydrogels where all samples contain 2 wt% nanoparticles. It was found that at all pH values, HA2 was the most swollen sample and HH2 was the least swollen one. This is likely due to presence of NH_2 groups in HA samples which resulted in more water absorption. However, NCC-HDTMS had hydrophobic surface which resulted in less water absorption in nanocomposite hydrogels. Moreover, as pH value increased, deprotonation of COOH functional groups of PAA were favored and the electrostatic repulsions between the COO^- anions caused the expansion of the hydrogel network and thus, swelling ratio (Kurdtabar et al. 2018; Nikravan et al. 2018a, b).

Figure S4 shows the effect of NCC content on the swelling ratio at different pH values. At first, higher amount of NCC led to higher swelling ratio due to hydrophilicity of cellulose nanocrystals (Lim and Ahmad 2014). However, at pH values equal to or

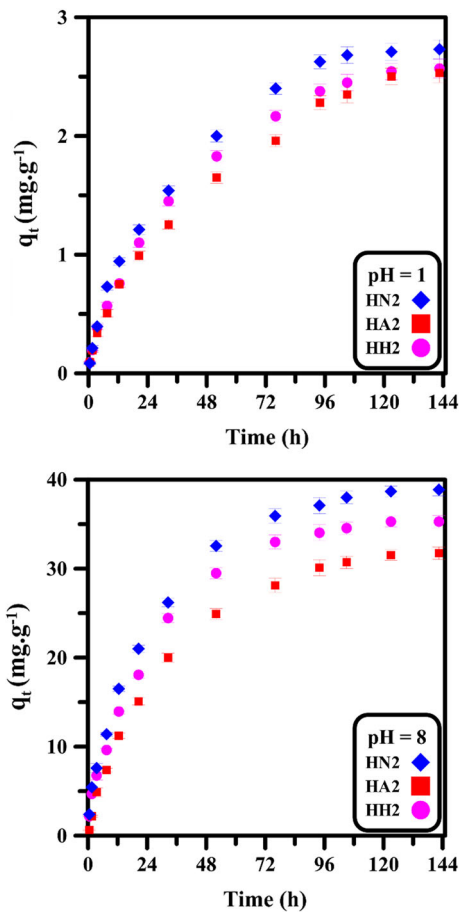


Fig. 5 Adsorption of MB versus time for HN2, HA2 and HH2 nanocomposite hydrogels at different pH values ($n = 3$, mean \pm SD)

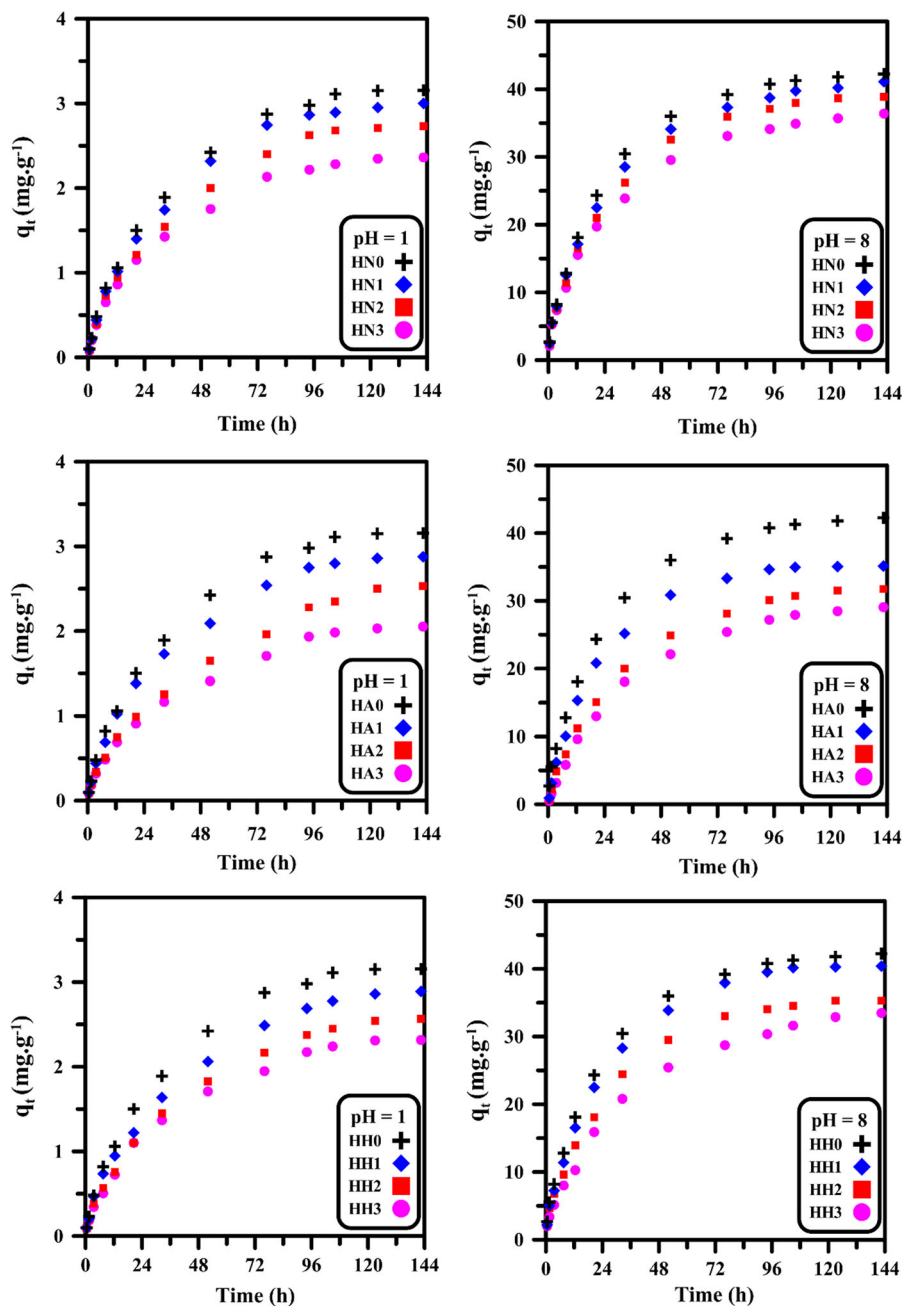
higher than pK_a value of PAA [$pK_a = 4.25$ (Lim et al. 2015)], carboxyl groups are partially or fully deprotonated which results in higher water absorption. In this state, strong hydrogen bonding between carboxyls of PAA and hydroxyls of NCC resulted in the more difficult penetration of water molecules into the structure. In the case of HA hydrogel nanocomposites (Figure S5), adding NCCs resulted in higher swelling ratio compared to neat hydrogel due to hydrophilic nature of NCC-APTES nanoparticles. However, adding more NCC-APTES nanoparticles resulted in decreasing swelling ratio. This can be attributed to the filling of the hydrogel network space with nanoparticles, which resulted in a more rigid hydrogel structure and subsequently, difficult water penetration into 3D structure of hydrogels (Lim et al. 2017). As depicted in Figure S6, an increase in the amount of

NCC-HDTMS nanoparticles resulted in lower swelling ratio even compared to neat hydrogel. This is attributed to hydrophobic surface of nanoparticles due to modification with HDTMS. Also, higher amount of nanoparticles resulted in a rigid structure of hydrogel nanocomposite and filled-space of 3D hydrogel network. This favored difficult water penetration and led to less swelling ratio.

Removal of MB by nanocomposite hydrogels

Pollution of surface and ground water with synthetic dyes is a significant environmental problem and is a threat to human life (Gupta et al. 2013). MB as an extensively-used dye causes different eye and skin injuries (Ghosh and Bhattacharyya 2002). However, because of its importance in industry, the adsorption capacity of MB by hydrogel nanocomposites is subject of work. Adsorption properties of the hydrogels were evaluated by means of UV-Vis. absorbance at 662.5 or 665 nm depending on pH of medium. Generally, removal of dyes by hydrogels are affected by (1) the surface charge of the adsorbent, (2) the degree of ionization of the adsorptive molecule and (3) extent of dissociation of functional groups on the active sites of the adsorbent (Crini 2006). The pH value of the dye solution is an important parameter in its adsorption by hydrogels. At higher pH values, carboxylic acid groups are ionized. So, electrostatic repulsions between COO^- groups leads to expanded structure of the hydrogels and increasing the interactions between negatively-charged groups in AA and positively-charged MB dye. Figure 5 shows the effect of pH value of the MB solution on the adsorption capacities of nanocomposite hydrogels containing 2 wt% of nanoparticles. It was found that as pH increased, the adsorption capacities increased for all samples. This can be explained by electrostatic interactions between MB and hydrogel structure. On the other hand, the $-\text{COOH}$ groups dissociated to form COO^- at higher pH values. Thus, carboxyl anions dominated the electrostatic repulsions between ionized groups leading to expansion of the hydrogels network and increasing adsorption capacity. Moreover, more deprotonated groups dominated interactions between cationic MB and hydrogel that resulted in higher adsorption capacity (Bulut and Karaer 2015). Surface modification of NCC also affected the adsorption capacity as shown in Fig. 5. According to

Fig. 6 Adsorption of MB versus time for HN, HA and HH nanocomposite hydrogels containing different amounts of nanoparticles at different pH values



the results, there is no significant difference between adsorption capacities by different samples at pH = 1. This originates from low swelling ratio of hydrogels that did not let MB to diffuse into 3D network. However, at pH = 8, HN2 nanocomposite hydrogel had the highest adsorption capacity whereas HA2 had the lowest one. This can be explained by presence of $-NH_2$ groups on the surface of NCC-APTES that can

prevent cationic dye adsorption via electrostatic repulsions.

Figure 6 shows that by incorporation and increasing the amount of all types of nanoparticles the adsorption capacity decreased at pH values of 1 and 8. This can be explained by filling the hydrogel structure by nanoparticles which did not permit to diffusion of dye from solution to 3D structure. However, by

Table 2 Adsorption kinetic parameters of pseudo-first-order model for MB adsorption onto hydrogels

Sample	pH = 1				pH = 8			
	q_e (exp.)	k_1 (h^{-1})	q_e (mg/g)	R^2	q_e (exp.)	k_1 (h^{-1})	q_e (mg/g)	R^2
HN0	3.15	0.042	3.90	0.921	42.24	0.035	38.75	0.998
HN1	3.00	0.033	3.07	0.995	41.10	0.030	36.12	0.998
HN2	2.73	0.037	3.12	0.967	38.88	0.037	38.86	0.975
HN3	2.36	0.035	2.53	0.961	36.40	0.030	32.50	0.996
HA1	2.88	0.037	3.24	0.958	35.12	0.049	39.88	0.981
HA2	2.53	0.029	2.83	0.913	31.74	0.036	34.67	0.963
HA3	2.05	0.033	2.25	0.956	29.06	0.030	29.79	0.995
HH1	2.89	0.032	3.14	0.961	40.41	0.045	44.47	0.978
HH2	2.57	0.032	2.84	0.948	35.28	0.036	33.73	0.999
HH3	2.32	0.038	2.79	0.892	33.48	0.028	34.15	0.977

Table 3 Adsorption kinetic parameters of pseudo-second-order model for MB adsorption onto hydrogels

Sample	pH = 1				pH = 8			
	q_e (exp.)	k_2 ($\text{g mg}^{-1} \text{h}^{-1}$)	q_e (mg/g)	R^2	q_e (exp.)	k_2 ($\text{g mg}^{-1} \text{h}^{-1}$)	q_e (mg/g)	R^2
HN0	3.15	0.010	3.80	0.993	42.24	0.001	47.13	0.996
HN1	3.00	0.010	3.60	0.993	41.10	0.001	45.58	0.995
HN2	2.73	0.001	3.28	0.989	38.88	0.001	43.59	0.994
HN3	2.36	0.015	2.76	0.993	36.40	0.001	40.28	0.994
HA1	2.88	0.011	3.43	0.992	35.12	0.001	41.05	0.998
HA2	2.53	0.010	3.05	0.968	31.74	0.001	38.68	0.998
HA3	2.05	0.015	2.42	0.982	29.06	0.001	37.07	0.998
HH1	2.89	0.010	3.45	0.987	40.41	0.001	46.08	0.994
HH2	2.57	0.011	3.09	0.983	35.28	0.001	40.16	0.992
HH3	2.32	0.013	2.77	0.986	33.48	0.001	38.54	0.984

varying the pH from 1 to 8, the adsorption capacity increased for all samples. For example, HN2 nanocomposite hydrogel showed equilibrium point at 2.6 mg/g at pH = 1 whereas at pH = 8, the equilibrium increased to 38 mg/g. This showed that the alkali media is better for MB adsorption because COOH groups are deprotonated and more interaction between the cationic dye and COO^- leads to increasing adsorption.

Adsorption kinetics

Prediction of adsorption kinetics is necessary for good understanding the adsorption mechanism. To investigate the adsorption mechanism of the nanocomposite hydrogels for MB dye in aqueous solutions, the

adsorption kinetics was analyzed. Three kinetic models were applied to fit the experimental data including pseudo-first-order (Eq. 5), pseudo-second-order (Eq. 6) and intra-particle diffusion (Eq. 7) models (Bulut and Karaer 2015; Chen and Wang 2009).

$$\ln(q_e - q_t) = \ln q_e - k_1 t \quad (5)$$

$$\frac{t}{q_t} = \frac{1}{q_e^2 k_2} + \frac{t}{q_e} \quad (6)$$

$$q_t = k_{id} t^{1/2} + C \quad (7)$$

where q_e and q_t (mg/g) represent the amount of dye adsorbed on nanocomposite hydrogels at equilibrium and any time respectively and k_1 (min^{-1} or h^{-1}) is rate constant. q_e and k_1 can be obtained by the intercept and

Table 4 Adsorption kinetic parameters of intra-particle diffusion model for MB adsorption onto hydrogels

Sample	pH	k_{i1}	C_1	R_1^2	k_{i2}	C_2	R_2^2
HN0	1	0.355	− 0.167	0.999	0.116	1.884	0.836
	8	4.856	0.146	0.982	0.735	33.680	0.986
HN1	1	0.339	− 0.169	0.999	0.062	2.262	0.997
	8	4.581	0.220	0.986	0.996	29.265	0.887
HN2	1	0.292	− 0.117	0.999	0.058	2.068	0.911
	8	4.361	0.112	0.990	1.105	26.493	0.960
HN3	1	0.258	− 0.080	0.997	0.091	1.336	0.982
	8	3.962	0.406	0.990	1.130	23.208	0.986
HA1	1	0.312	− 0.121	0.996	0.078	1.994	0.995
	8	4.315	− 0.182	0.979	0.286	31.930	0.838
HA2	1	0.238	− 0.100	0.999	0.160	0.721	0.992
	8	3.605	− 1.803	0.993	1.012	20.311	0.998
HA3	1	0.206	− 0.055	0.998	0.068	1.277	0.984
	8	3.319	− 2.340	0.992	0.894	18.602	0.957
HH1	1	0.302	− 0.119	0.999	0.121	1.520	0.982
	8	4.697	− 0.585	0.988	0.511	34.698	0.773
HH2	1	0.267	− 0.126	0.997	0.120	1.219	0.997
	8	4.035	− 0.445	0.992	0.888	25.436	1.000
HH3	1	0.245	− 0.101	0.992	0.098	1.232	0.988
	8	3.565	− 1.066	0.990	1.782	13.178	0.988

slope of $\ln(q_e - q_t)$ versus t (h) (Figure S7). k_2 (g/(mg h)) is the pseudo second-order rate constant where q_e and k_2 can be calculated from the slope and intercept of t/q_t against t (h) (Figure S8). k_{id} (mg/(g h^{1/2})) is the intra-particle diffusion rate parameter where plot of q_t against $t^{1/2}$ should be a straight line with a slope of k_{id} and intercept of C (Figure S9). The calculated q_e , k_1 , k_2 , k_{id} , C and the corresponding linear regression correlation coefficient (R^2) are summarized in Tables 2, 3 and 4. It can be concluded that both pseudo-first-order model and pseudo-second-order model have good correlation coefficients for MB dye, but the pseudo-second-order model have a better fitting data. Also, difference of q_e values between the experiment and calculated values at pseudo second-order model is slightly higher than pseudo-first-order model.

Intra-particle diffusion model showed that the adsorption mechanism for dye had two separate phases due to the appearance of the two sections with variant linear slopes; the first sharper segment is due to the transportation of dye molecules from the bulk solution to the external surface of the hydrogels by diffusion through the boundary layer (film diffusion), and the second portion comes from the equilibrium

stage as the dye concentration was very low. It was found that the correlation coefficient for the intra-particle diffusion model is lower than the pseudo-first-order and the pseudo-second-order models. This indicates that the intra-particle diffusion model is not appropriate for adsorption of MB onto the nanocomposite hydrogels.

Conclusions

In this study, we prepared a series of PAA/(modified) NCC nanocomposite hydrogels containing different amounts of (modified) NCCs using free radical polymerization in the presence of MBA as cross-linker. At first, we modified NCC with APTES and HDTMS. Then, the free radical polymerization was performed to produce nanocomposite hydrogels those were used for adsorption of MB dye. HA nanocomposites showed the most swollen state whereas HH ones had the least SR due to existence of hydrophilic NH₂ groups in HA samples and hydrophobic surface of nanoparticles in HH nanocomposites. Moreover, higher pH values favored deprotonation of COOH functional groups of PAA and the electrostatic

repulsions between the COO^- anions which caused higher SR. MB adsorption of the hydrogels showed that removal of MB were affected by the surface nature of nanoparticles, pH value of medium and amount of nanoparticles. It was found that as pH increased, the adsorption capacities increased for all samples because more deprotonated groups dominated interactions between cationic MB and hydrogel. However, HN nanocomposite hydrogels had the highest adsorption capacity whereas HA samples had the lowest one due to presence of $-\text{NH}_2$ groups on the surface of NCC-APTES that can prevent cationic dye adsorption via electrostatic repulsions.

Funding This research did not receive any specific grant from funding agencies in the public, commercial, or not-for-profit sectors.

Compliance with ethical standards

Conflict of interest The authors declare that they have no conflict of interest.

References

- Abdeen Z, Mohammad SG (2014) Study of the adsorption efficiency of an eco-friendly carbohydrate polymer for contaminated aqueous solution by organophosphorus pesticide. *Open J Org Polym Mater* 4:16–28. <https://doi.org/10.4236/ojopm.2014.41004>
- Abdollahi E, Abdouss M, Salami-Kalajahi M, Mohammadi A (2016) Molecular recognition ability of molecularly imprinted polymer nano- and micro-particles by reversible addition-fragmentation chain transfer polymerization. *Polym Rev* 56:557–583. <https://doi.org/10.1080/15583724.2015.1119162>
- Abdollahi E, Khalafi-Nezhad A, Mohammadi A, Abdouss M, Salami-Kalajahi M (2018) Synthesis of new molecularly imprinted polymer via reversible addition fragmentation transfer polymerization as a drug delivery system. *Polymer* 143:245–257. <https://doi.org/10.1016/j.polymer.2018.03.058>
- Ahmad A, Rafatullah M, Sulaiman O, Ibrahim MH, Hashim R (2009) Scavenging behaviour of meranti sawdust in the removal of methylene blue from aqueous solution. *J Hazard Mater* 170:357–365. <https://doi.org/10.1016/j.jhazmat.2009.04.087>
- Ahvenainen P, Kontro I, Svedström K (2016) Comparison of sample crystallinity determination methods by X-ray diffraction for challenging cellulose I materials. *Cellulose* 23:1073–1086. <https://doi.org/10.1007/s10570-016-0881-6>
- Akkaya MÇ, Emik S, Güçlü G, İyim TB, Özgümüş S (2009) Removal of basic dyes from aqueous solutions by crosslinked-acrylic acid/acrylamidopropane sulfonic acid hydrogels. *J Appl Polym Sci* 114:1150–1159. <https://doi.org/10.1002/app.30704>
- Almeida CAP, Debacher NA, Downs AJ, Cottet L, Mello CAD (2009) Removal of methylene blue from colored effluents by adsorption on montmorillonite clay. *J Colloid Interface Sci* 332:46–53. <https://doi.org/10.1016/j.jcis.2008.12.012>
- Amirshaqai N, Salami-Kalajahi M, Mahdavian M (2014) Corrosion behavior of aluminum/silica/polystyrene nanostructured hybrid flakes. *Iran Polym J* 23:699–706. <https://doi.org/10.1007/s13726-014-0264-5>
- Anirudhan TS, Rejeena SR (2012) Poly (acrylic acid)-modified poly (glycidylmethacrylate)-grafted nanocellulose as matrices for the adsorption of lysozyme from aqueous solutions. *Chem Eng J* 187:150–159. <https://doi.org/10.1016/j.cej.2012.01.113>
- Annadurai G, Juang R, Lee DJ (2002) Use of cellulose-based wastes for adsorption of dyes from aqueous solutions. *J Hazard Mater* 92:263–274. [https://doi.org/10.1016/S0304-3894\(02\)00017-1](https://doi.org/10.1016/S0304-3894(02)00017-1)
- Atta AM, Ismail HS, Elsaad AM (2012) Application of anionic acrylamide-based hydrogels in the removal of heavy metals from waste water. *J Appl Polym Sci* 123:2500–2510. <https://doi.org/10.1002/app.34798>
- Banaei M, Salami-Kalajahi M (2015) Synthesis of poly(2-hydroxyethyl methacrylate)-grafted poly(aminoamide) dendrimers as polymeric nanostructures. *Colloid Polym Sci* 293:1553–1559. <https://doi.org/10.1007/s00396-015-3559-y>
- Bashir S, Teo YY, Naeem S, Ramesh S, Ramesh K (2017) pH responsive N-succinyl chitosan/poly(acrylamide-co-acrylic acid) hydrogels and in vitro release of 5-fluorouracil. *PLoS ONE* 12:e0179250. <https://doi.org/10.1371/journal.pone.0179250>
- Bekiari V, Sotiropoulou M, Bokias G, Lianos P (2008) Use of poly(N, Ndimethylacrylamide-co-sodium acrylate) hydrogel to extract cationic dyes and metals from water. *Colloids Surf Physicochem Eng Asp* 312:214–218. <https://doi.org/10.1016/j.colsurfa.2007.06.053>
- Bhatia M, Rajulapati SB, Sonawane S, Girdhar A (2017) Synthesis and implication of novel poly (acrylic acid)/nanosorbent embedded hydrogel composite for lead ion removal. *Sci Rep* 7:16413. <https://doi.org/10.1038/s41598-017-15642-9>
- Blus K, Czechowski J, Koziróg A (2014) New eco-friendly method for paper dyeing. *Fibres Text East Eur* 22:121–125
- Bulut Y, Karaer H (2015) Removal of methylene blue from aqueous solution by crosslinked chitosan-g-poly(acrylic acid)/bentonite composite. *Chem Eng Commun* 202:1635–1644. <https://doi.org/10.1080/00986445.2014.968713>
- Cha R, He Z, Ni Y (2012) Preparation and characterization of thermal/pH-sensitive hydrogel from carboxylated nanocrystalline cellulose. *Carbohydr Polym* 88:713–718. <https://doi.org/10.1016/j.carbpol.2012.01.026>
- Chen H, Wang A (2009) Adsorption characteristics of Cu(II) from aqueous solution onto poly(acrylamide)/attapulgite composite. *J Hazard Mater* 165:223–231. <https://doi.org/10.1016/j.jhazmat.2008.09.097>
- Cheng HL, Feng QH, Liao CA, Liu Y, Wu DB, Wang QG (2016) Removal of methylene blue with

- hemicellulose/clay hybrid hydrogels. *Chin J Polym Sci* 34:709–719. <https://doi.org/10.1007/s10118-016-1788-2>
- Ciardelli G, Corsi L, Marcucci M (2001) Membrane separation for wastewater reuse in the textile industry. *Resour Conserv Recycl* 31:189–197. [https://doi.org/10.1016/S0921-3449\(00\)00079-3](https://doi.org/10.1016/S0921-3449(00)00079-3)
- Crini G (2006) Non-conventional low-cost adsorbents for dye removal: a review. *Bioresour Technol* 97:1061–1085. <https://doi.org/10.1016/j.biortech.2005.05.001>
- de Paiva SD, da Silva IB, de Moura Santos ECM, Rocha IMV, Martínez-Huitle CA, dos Santos EV (2018) Coupled Electrochemical Processes for Removing Dye from Soil and Water. *J Electrochem Soc* 165:E318–E324. <https://doi.org/10.1149/2.0391809jes>
- Dehghani E, Salami-Kalajahi M, Roghani-Mamaqani H (2019) Fabricating cauliflower-like and dumbbell-like Janus particles: loading and simultaneous release of DOX and ibuprofen. *Colloids Surf B-Biointerfaces* 173:155–163. <https://doi.org/10.1016/j.colsurfb.2018.09.068>
- Fallahi-Sambaran M, Salami-Kalajahi M, Dehghani E, Abbasi F (2018) Investigation of different core-shell toward Janus morphologies by variation of surfactant and feeding composition: a study on the kinetics of DOX release. *Colloids Surf B-Biointerfaces* 170:578–587. <https://doi.org/10.1016/j.colsurfb.2018.06.064>
- Fallahi-Sambaran M, Salami-Kalajahi M, Dehghani E, Abbasi F (2019) Investigating Janus morphology development of poly(acrylic acid)/poly(2-(dimethylamino)ethyl methacrylate) composite particles: an experimental study and mathematical modeling of DOX release. *Microchem J* 145:492–500. <https://doi.org/10.1016/j.microc.2018.11.017>
- Gao Q, Zhu Q, Yang CQ (2009) Formation of highly hydrophobic surfaces on cotton and polyester fabrics using silica sol nanoparticles and nonfluorinated alkylsilane. *Ind Eng Chem Res* 48:9797–9803. <https://doi.org/10.1021/ie9005518>
- Ghosh D, Bhattacharyya KG (2002) Adsorption of methylene blue on kaolinite. *Appl Clay Sci* 20:295–300. [https://doi.org/10.1016/S0169-1317\(01\)00081-3](https://doi.org/10.1016/S0169-1317(01)00081-3)
- Golshan M, Salami-Kalajahi M, Roghani-Mamaqani H, Mohammadi M (2017) Poly(propylene imine) dendrimer-grafted nanocrystalline cellulose: doxorubicin loading and release behavior. *Polymer* 117:287–294. <https://doi.org/10.1016/j.polymer.2017.04.047>
- Guerra E, Llompert M, Garcia-Jares C (2018) Analysis of dyes in cosmetics: challenges and recent developments. *Cosmetics* 5:47. <https://doi.org/10.3390/cosmetics5030047>
- Gupta VK, Kumar R, Nayak A, Saleh TA, Barakat MA (2013) Adsorptive removal of dyes from aqueous solution onto carbon nanotubes: a review. *Adv Colloid Interface Sci* 193:24–34. <https://doi.org/10.1016/j.cis.2013.03.003>
- Habibi Y (2014) Key advances in the chemical modification of nanocelluloses. *Chem Soc Rev* 43:1519–1542. <https://doi.org/10.1039/C3CS60204D>
- Haqani M, Roghani-Mamaqani H, Salami-Kalajahi M (2017) Synthesis of dual-sensitive nanocrystalline cellulose-grafted block copolymers of N-isopropylacrylamide and acrylic acid by reversible addition-fragmentation chain transfer polymerization. *Cellulose* 24:2241–2254. <https://doi.org/10.1007/s10570-017-1249-2>
- Hernandez-Martínez AR, Lujan-Montelongo JA, Silva-Cuevas C, Mota-Morales JD, Cortez-Valadez M, de Jesus Ruíz-Baltazar A, Cruz M, Herrera-Ordóñez J (2018) Swelling and methylene blue adsorption of poly (N, N-dimethylacrylamide-co-2-hydroxyethyl methacrylate) hydrogel. *React Funct Polym* 122:75–84. <https://doi.org/10.1016/j.reactfunctpolym.2017.11.008>
- Hou K, Li Y, Liu Y, Zhang R, Hsiao BS, Zhu M (2017) Continuous fabrication of cellulose nanocrystal/poly (ethylene glycol) diacrylate hydrogel fiber from nanocomposite dispersion: rheology, preparation and characterization. *Polymer* 123:55–64. <https://doi.org/10.1016/j.polymer.2017.06.034>
- Ibrahim SM, El Salmawi KM, Zahran AH (2007) Synthesis of crosslinked superabsorbent carboxymethyl cellulose/acrylamide hydrogels through electron-beam irradiation. *J Appl Polym Sci* 104:2003–2008. <https://doi.org/10.1002/app.25916>
- Kargarzadeh H, Ahmad I, Abdullah I, Dufresne A, Zainudin SY, Sheltami RM (2012) Effects of hydrolysis conditions on the morphology, crystallinity, and thermal stability of cellulose nanocrystals extracted from kenaf bast fibers. *Cellulose* 19:855–866. <https://doi.org/10.1007/s10570-012-9684-6>
- Kaşgöz H, Durmus A (2008) Dye removal by a novel hydrogel-clay nanocomposite with enhanced swelling properties. *Polym Adv Technol* 19:838–845. <https://doi.org/10.1002/pat.1045>
- Kumar A, Negi YS, Choudhary V, Bhardwaj NK (2014) Characterization of cellulose nanocrystals produced by acid-hydrolysis from sugarcane bagasse as agro-waste. *J Mater Phys Chem* 2:1–8. <https://doi.org/10.12691/jmpc-2-1-1>
- Kurdtabar M, Koutenae RN, Bardajee GR (2018) Synthesis and characterization of a novel pH-responsive nanocomposite hydrogel based on chitosan for targeted drug release. *J Polym Res* 25:119. <https://doi.org/10.1007/s10965-018-1499-1>
- Li S, Zhang H, Feng J, Xu R, Liu X (2011) Facile preparation of poly (acrylic acid-acrylamide) hydrogels by frontal polymerization and their use in removal of cationic dyes from aqueous solution. *Desalination* 280:95–102. <https://doi.org/10.1016/j.desal.2011.06.056>
- Lim LS, Ahmad I (2014) Chemical crosslinking of acrylic acid to form biocompatible pH sensitive hydrogel reinforced with cellulose nanocrystals (CNC). *AIP Conf Proc* 1614:366–370. <https://doi.org/10.1063/1.4895224>
- Lim LS, Ahmad I, Lazim MASM (2015) pH sensitive hydrogel based on poly(acrylic acid) and cellulose nanocrystals. *Sains Malaysiana* 44:779–785. <https://doi.org/10.17576/jsm-2015-4406-02>
- Lim LS, Rosli NA, Ahmad I, Lazim MASM, Amin MCIM (2017) Synthesis and swelling behavior of pH-sensitive semi-IPN superabsorbent hydrogels based on poly (acrylic acid) reinforced with cellulose nanocrystals. *Nanomaterials* 7:399. <https://doi.org/10.3390/nano7110399>
- Liu Y, Zheng Y, Wang A (2010) Enhanced adsorption of Methylene Blue from aqueous solution by chitosan-g-poly (acrylic acid)/vermiculite hydrogel composites. *J Environ Sci* 22:486–493. [https://doi.org/10.1016/S1001-0742\(09\)60134-0](https://doi.org/10.1016/S1001-0742(09)60134-0)

- Liu J, Liu G, Liu W (2014) Preparation of water-soluble β -cyclodextrin/poly(acrylic acid)/graphene oxide nanocomposites as new adsorbents to remove cationic dyes from aqueous solutions. *Chem Eng J* 25:299–308. <https://doi.org/10.1016/j.cej.2014.07.021>
- Lu B, Tarn MD, Pamme N, Georgiou TK (2015a) Tailoring pH-responsive acrylic acid microgels with hydrophobic crosslinks for drug release. *J Mater Chem* 3:4524–4529. <https://doi.org/10.1039/C5TB00222B>
- Lu T, Xiang T, Huang XL, Li C, Zhao WF, Zhang Q, Zhao CS (2015b) Post-crosslinking towards stimuli-responsive sodium alginate beads for the removal of dye and heavy metals. *Carbohydr Polym* 133:587–595. <https://doi.org/10.1016/j.carbpol.2015.07.048>
- Luo X, Zhang L (2009) High effective adsorption of organic dyes on magnetic cellulose beads entrapping activated carbon. *J Hazard Mater* 171:340–347. <https://doi.org/10.1016/j.jhazmat.2009.06.009>
- Luo JH, Li YY, Wang PM, Xia BB, He LP, Yang BW, Jiang B (2017) A facial route for preparation of hydrophobic nanosilica modified by silane coupling agents. *Key Eng Mater* 727:353–358. <https://doi.org/10.4028/www.scientific.net/KEM.727.353>
- Luo M-T, Li H-L, Huang C, Zhang H-R, Xiong L, Chen X-F, Chen X-D (2018) Cellulose-based absorbent production from bacterial cellulose and acrylic acid: synthesis and performance. *Polymers* 10:702. <https://doi.org/10.3390/polym10070702>
- Maiti S, Jayaramudu J, Das K, Reddy SM, Sadiku R, Ray SS, Liu D (2013) Preparation and characterization of nanocellulose with new shape from different precursor. *Carbohydr Polym* 98:562–567. <https://doi.org/10.1016/j.carbpol.2013.06.029>
- Malik PK, Saha SK (2003) Oxidation of direct dyes with hydrogen peroxide using ferrous ion as catalyst. *Sep Purif Technol* 31:241–250. [https://doi.org/10.1016/S1383-5866\(02\)00200-9](https://doi.org/10.1016/S1383-5866(02)00200-9)
- Mall ID, Srivastava VC, Agarwal NK, Mishra IM (2005) Removal of congo red from aqueous solution by bagasse fly ash and activated carbon: kinetic study and equilibrium isotherm analyses. *Chemosphere* 61:492–501. <https://doi.org/10.1016/j.chemosphere.2005.03.065>
- Mazlita Y, Lee HV, Hamid SBA (2016) Preparation of cellulose nanocrystals bio-polymer from agro-industrial wastes: separation and characterization. *Polym Polym Compos* 24:719–728. <https://doi.org/10.1177/096739111602400907>
- Melo BC, Paulino FA, Cardoso VA, Pereira AG, Fajardo AR, Rodrigues FH (2018) Cellulose nanowhiskers improve the methylene blue adsorption capacity of chitosan-g-poly(acrylic acid) hydrogel. *Carbohydr Polym* 181:358–367. <https://doi.org/10.1016/j.carbpol.2017.10.079>
- Modarresi-Saryazdi SM, Haddadi-Asl V, Salami-Kalajahi M (2018) *N,N'*-methylenebis(acrylamide)-crosslinked poly(acrylic acid) particles as doxorubicin carriers: a comparison between release behavior of physically loaded drug and conjugated drug via acid-labile hydrazone linkage. *J Biomed Mater Res A* 106:342–348. <https://doi.org/10.1002/jbm.a.36240>
- Moqadam S, Salami-Kalajahi M, Mahdavian M (2018) Synthesis and characterization of sunflower oil-based polysulfide polymer/cloisite 30B nanocomposites. *Iran J Chem Eng* 37:185–192
- Nath J, Dolui SK (2018) Synthesis of carboxymethyl cellulose-g-poly(acrylic acid)/LDH hydrogel for in vitro controlled release of vitamin B₁₂. *Appl Clay Sci* 155:65–73. <https://doi.org/10.1016/j.clay.2018.01.004>
- Nikravan G, Haddadi-Asl V, Salami-Kalajahi M (2018a) Synthesis of pH-responsive magnetic yolk-shell nanoparticles: a comparison between the conventional etching and new deswelling approaches. *Appl Organometal Chem* 32:e4272. <https://doi.org/10.1002/aoc.4272>
- Nikravan G, Haddadi-Asl V, Salami-Kalajahi M (2018b) Synthesis of dual temperature- and pH-responsive yolk-shell nanoparticles by conventional etching and new deswelling approaches: DOX release behavior. *Colloids Surf B-Biointerfaces* 165:1–8. <https://doi.org/10.1016/j.colsurfb.2018.02.010>
- Nilsson C (2017) Preparation and characterization of nanocellulose from wheat bran, Lund University. <http://lup.lub.lu.se/student-papers/record/8906333>
- Noein L, Haddadi-Asl V, Salami-Kalajahi M (2017) Grafting of pH-sensitive poly(*N,N*-dimethylaminoethyl methacrylate-co-2-hydroxyethyl methacrylate) onto halloysite nanotubes via surface-initiated atom transfer radical polymerization for controllable drug release. *Int J Polym Mater Polym Biomater* 66:123–131. <https://doi.org/10.1080/00914037.2016.1190927>
- Panahian P, Salami-Kalajahi M, Hosseini MS (2014) Synthesis of dual thermoresponsive and pH-sensitive hollow nanospheres by atom transfer radical polymerization. *J Polym Res* 21:455. <https://doi.org/10.1007/s10965-014-0455-y>
- Panswed J, Wongchaisuwan S (1986) Mechanisms of dye wastewater colour removal by magnesium carbonate-hydrated basic. *Water Sci Technol* 18:139–144. <https://doi.org/10.2166/wst.1986.0045>
- Patil PS, Phugare SS, Jadhav SB, Jadhav JP (2010) Communal action of microbial cultures for Red HE3B degradation. *J Hazard Mater* 181:263–270. <https://doi.org/10.1016/j.carbpol.2013.05.093>
- Pirayesh A, Salami-Kalajahi M, Roghani-Mamaqani H, Dehghani E (2018) Amine-modified graphene oxide as co-curing agent of epoxidized polysulfide prepolymer: thermophysical and mechanical properties of nanocomposites. *Diamond Relat Mater* 86:109–116. <https://doi.org/10.1016/j.diamond.2018.04.025>
- Qi X, Wu L, Su T, Zhang J, Dong W (2018) Polysaccharide-based cationic hydrogels for dye adsorption. *Colloids Surf B-Biointerfaces* 170:364–372. <https://doi.org/10.1016/j.colsurfb.2018.06.036>
- Rahchamani J, Mousavi HZ, Behzad M (2011) Adsorption of methyl violet from aqueous solution by polyacrylamide as an adsorbent: isotherm and kinetic studies. *Desalination* 267:256–260. <https://doi.org/10.1016/j.desal.2010.09.036>
- Rashidzadeh A, Olad A, Salari D (2015) The effective removal of methylene blue dye from aqueous solutions by NaAlg-g-poly(acrylic acid-co-acryl amide)/clinoptilolite hydrogel nanocomposite. *Fib Polym* 16:354–362. <https://doi.org/10.1007/s12221-015-0354-9>
- Seema HS, Deepika L, Ambika B (2018) a comparative study on discharge printing using conventional and ecological recipe. *Trends Text Eng Fashion Technol*

- 3:TTEFT.000552.2018. <https://doi.org/10.31031/TTEFT.2018.03.000552>
- Segal L, Creely JJ, Martin AE, Conrad CM (1959) An empirical method for estimating the degree of crystallinity of native cellulose using the X-ray diffractometer. *Text Res J* 29:786–794. <https://doi.org/10.1177/004051755902901003>
- Shankar S, Rhim JW (2016) Preparation of nanocellulose from micro-crystalline cellulose: the effect on the performance and properties of agar-based composite films. *Carbohydr Polym* 135:18–26. <https://doi.org/10.1016/j.carbpol.2015.08.082>
- Sharifzadeh E, Salami-Kalajahi M, Hosseini MS, Aghjeh MKR (2016) A temperature-controlled method to produce Janus nanoparticles using high internal interface systems: experimental and theoretical approaches. *Colloids Surf A Physicochem Eng Asp* 506:56–62. <https://doi.org/10.1016/j.colsurfa.2016.06.006>
- Sharma R, Kaith BS, Kalia S, Pathania D, Kumar A, Sharma N, Street RM, Schauer C (2015) Biodegradable and conducting hydrogels based on Guar gum polysaccharide for antibacterial and dye removal applications. *J Environ Manag* 162:37–45. <https://doi.org/10.1016/j.jenvman.2015.07.044>
- Singh T, Singhal R (2015) Kinetics and thermodynamics of cationic dye adsorption onto dry and swollen hydrogels pol (acrylic acid-sodium acrylate-acrylamide) sodium humate. *Desalin Water Treat* 53:3668–3680. <https://doi.org/10.1080/19443994.2013.871342>
- Soleimani K, Tehrani AD, Adeli ADM (2018) Bioconjugated graphene oxide hydrogel as an effective adsorbent for cationic dyes removal. *Ecotoxicol Environ Saf* 147:34–42. <https://doi.org/10.1016/j.ecoenv.2017.08.021>
- Şolpan D, Duran S, Saraydin D, Güven O (2003) Adsorption of methyl violet in aqueous solutions by poly(acrylamide-co-acrylic acid) hydrogels. *Rad Phys Chem* 66:117–127. [https://doi.org/10.1016/S0969-806X\(02\)00384-5](https://doi.org/10.1016/S0969-806X(02)00384-5)
- Suo A, Qian J, Yao Y, Zhang W (2007) Synthesis and properties of carboxymethyl cellulose-graft-poly (acrylic acid-co-acrylamide) as a novel cellulose-based superabsorbent. *J Appl Polym Sci* 103:1382–1388. <https://doi.org/10.1002/app.23948>
- Vakili M, Rafatullah M, Salamatinia B, Abdullah AZ, Ibrahim MH, Tan KB, Amouzgar P (2014) Application of chitosan and its derivatives as adsorbents for dye removal from water and wastewater. *Carbohydr Polym* 113:115–130. <https://doi.org/10.1016/j.carbpol.2014.07.007>
- Varaprasad K, Jayaramudu T (2017) Removal of dye by carboxymethyl cellulose, acrylamide and graphene oxide via a free radical polymerization process. *Carbohydr Polym* 164:186–194. <https://doi.org/10.1016/j.carbpol.2017.01.094>
- Wang S, Peng Y (2010) Natural zeolites as effective adsorbents in water and wastewater treatment. *Chem Eng J* 156:11–24. <https://doi.org/10.1016/j.cej.2009.10.029>
- Wang J, Wang W, Wang A (2010) Synthesis, characterization and swelling behaviors of hydroxyethyl cellulose-g-poly(acrylic acid)/attapulgit superabsorbent composite. *Polym Eng Sci* 50:1019–1027. <https://doi.org/10.1002/pen.21500>
- Yamada K, Yoshii S, Kumagai S, Fujiwara I, Nishio K, Okuda M, Matsukawa N, Yamashita I (2006) High-density and highly surface selective adsorption of protein–nanoparticle complexes by controlling electrostatic interaction. *Jpn J Appl Phys* 45:4259. <https://doi.org/10.1143/JJAP.45.4259>
- Yang J (2017) Manufacturing of nanocrystalline cellulose. Aalto University. <http://urn.fi/URN:NBN:fi:aalto-201709046803>
- Yang J, Han CR, Duan JF, Ma MG, Zhang XM, Xu F, Sun RC, Xie XM (2012) Studies on the properties and formation mechanism of flexible nanocomposite hydrogels from cellulose nanocrystals and poly(acrylic acid). *J Mater Chem* 22:22467–22480. <https://doi.org/10.1039/C2JM35498E>
- Yassin S, Su K, Lin H, Gladden LF, Zeitler JA (2015) Diffusion and swelling measurements in pharmaceutical powder compacts using terahertz pulsed imaging. *J Pharm Sci* 104:1658–1667. <https://doi.org/10.1002/jps.24376>
- Yetimoğlu K, Kahraman MV, Ercan O, Akdemir ZS, Apohan NK (2007) Nvinylpyrrolidone/acrylic acid/2-acrylamido-2-methylpropane sulfonic acid based hydrogels: synthesis, characterization and their application in the removal of heavy metals. *React Funct Polym* 67:451–460. <https://doi.org/10.1016/j.reactfunctpolym.2007.02.007>
- Zarezaeh-Mehrzi M, Karimi M, Qomi M (2017) Removal of methylene blue using polyacrylic acid/octavinyl polyhedral oligomeric silsesquioxane nanocomposite. *J Nanoanalysis* 4:134–141. <https://doi.org/10.22034/jna.2017.02.006>
- Zendeheel M, Barati A, Alikhani H, Hekmat A (2010) Removal of methylene blue dye from wastewater by adsorption onto semi-impenetrating polymer network hydrogels composed of acrylamide and acrylic acid copolymer and polyvinyl alcohol. *Iran J Environ Health Sci Eng* 7:431–436
- Zhang H, Song SP, She Y, Lang Q, Pu JW (2012) Modification of NCC for Improving the wetting property with polyurethane. *Adv Mater Res* 528:164–167. <https://doi.org/10.4028/www.scientific.net/AMR.528.164>
- Zheng Y, Wang A (2009) Evaluation of ammonium removal using a chitosan-g-poly (acrylic acid)/rectorite hydrogel composite. *J Hazard Mater* 171:671–677. <https://doi.org/10.1016/j.jhazmat.2009.06.05>
- Zhou Y, Fu S, Liu H, Yang S, Zhan H (2011) Removal of methylene blue dyes from wastewater using cellulose-based superadsorbent hydrogels. *Polym Eng Sci* 51:2417–2424. <https://doi.org/10.1002/pen.22020>

Publisher's Note Springer Nature remains neutral with regard to jurisdictional claims in published maps and institutional affiliations.